University of Baghdad
College of Engineering
JOURNAL OF ENGINEERING

Journal of Engineering
journal homepage: www.joe.uobaghdad.edu.iq
Number 1 Volume 28 January 2022

Civil and Architectural Engineering

Serviceability of Post-fire RC Rafters with Openings of Different Sizes and Shapes

Bashar F. Abdulkareem
Asst. Lect.
Department of Civil Engineering
University of Baghdad
Baghdad-Iraq
bashar.faisal@muc.edu.iq

Amer F. Izzat
Prof. Dr.
Department of Civil Engineering
University of Baghdad
Baghdad-Iraq
amer.f@coeng.uobaghdad.edu.iq

ABSTRACT

This study deals with the serviceability of reinforced concrete solid and perforated rafters with openings of different shapes and sizes based on an experimental study that includes 12 post-fire non-prismatic reinforced concrete beams (solid and perforated). Three groups were formed based on heating temperature (room temperature, 400 °C, and 700 °C), each group consisting of four rafters (solid, rafters with 6 and 8 trapezoidal openings, and rafter with eight circular openings) under static loading. A developed unified calculation technique for deflection and crack widths under static loading at the service stage has been provided, which comprises non-prismatic beams with or without opening exposed to flexure concentrated force. Two approaches were used to compute the deflection: The first attempt was conducted by using the moment of inertia for solid non-prismatic beam and reduced for those with openings by the ratio of residual rafter self-weight. The second was performed by using the moment of inertia of transformed cracked sections depending on the segmental rafter method. The crack width was determined using the ACI code's equation. The analytical and experimental results were evaluated and found to be in good agreement.

Keywords: ASTM E-119; reinforced concrete rafter; crack width; deflection; burning temperature.

خدمية العتبات الجملونية الخرسانية المسلحة والمزودة بفتحات مختلفة الشكل والابعاد بعد الحرق

بشار فيصل عبد الكريم
مدرس مساعد
جامعة بغداد كلية الهندسة

د. عامر فاروق عزت
استاذ
جامعة بغداد كلية الهندسة

الخلاصة

تتناول هذه الدراسة القابلية الخدمية للعتبات الجملونية الخرسانية المسلحة الصلبة والمثقبة والمزودة بفتحات بأشكال وأحجام مختلفة ، على أساس دراسة تجريبية تضم 12 عتبة من الخرسانة المسلحة غير المنشورية بعد الحريق (صلبة ومثقبة). تم تشكيل

*Corresponding author
Peer review under the responsibility of University of Baghdad.
https://doi.org/10.31026/j.eng.2022.01.02

Article received: 2/9/2021
Article accepted: 3 /10/2021
Article published:1/1/2022

ثلاث مجموعات على أساس درجة حرارة التسخين (درجة حرارة الغرفة ، 400 درجة مئوية ، و 700 درجة مئوية) ، كل مجموعة تتكون من أربعة عتبات (صلبة ، عتبات مع 6 و 8 فتحات شبه منحرفة ، وعتبات ذات 8 فتحات دائرية) تحت التحميل الساكن. تم توفير تقنية حساب موحدة مطورة للهطول وعرض الشقوق تحت التحميل الساكن في مرحلة الخدمية ، والتي تشتمل على عتبات جملونية مع أو بدون فتحة معرضة لقوة مركزة للثني. تم استخدام طريقتين لحساب الهطول : تم إجراء المحاولة الأولى باستخدام عزم القصور الذاتي للعتبة الصلبة وتم تقليلها بالنسبة لأولئك الذين لديهم فتحات بنسبة الوزن الذاتي للعتبات المثقبة المتبقية ، والمحاولة الثانية ، تم إجراؤها باستخدام عزم القصور الذاتي والناتج من تحويل المقاطع المتشققة اعتمادًا على طريقة الجمالون القطاعي. تم تحديد عرض الكراك باستخدام معادلة الكودالامريكي . تم تقييم النتائج التحليلية والتجريبية ووجد ان بينهما توافق جيد.

الكلمات الرئيسية: ASTM E-119 , العتبات الجملونية الخرسانية المسلحة ,عرض الشق , الانحراف , درجة حرارة الحرق.

1. INTRODUCTION

Because concrete has a comparatively cheap material cost, a strong reputation for excellent fire resistance, and low maintenance requirements, RC rafters can be utilized as an alternate preferable choice to support broad area roofs of warehouses, industrial buildings, and aviation hangars. Fire resistance analysis is an essential component of any fire safety design. The goal is to guarantee that the fire-resistant design is greater than the severity of the fire. Standard fire resistance tests are the most frequent technique of testing structural components' fire resistance.

(Hassan, et al., 2020) submitted experimental and numerical research evaluating the impact of various layouts of openings on the flexural performance of RC rafters. A nonlinear F.E. software, ABAQUS (2018), was used to validate the results of the tested rafters. Experiments have been carried out in the past to emphasize the influence of fires on the material characteristics of concrete with different mix amounts under different fire situations **(Chang et al., 2006); (Handoo and Agarwal, 2002); (Lee Xi and Willam, 2008); and (Tufail et al., 2017)**. Although concrete has a limited heat conductivity, **(Georgali and Tsakiridis, 2005)** found that it may sustain significant damage when exposed to heat. The finding of the heating history of concrete is important for forensic investigation or determining perhaps the concrete building exposed to fire, and its components are structurally intact. Visual examinations of cracking, discoloration, and spalling are routinely used to assess the fire damage of concrete structures. **(Wickstrom, U., 1986)** created one of the earliest models; this "extremely basic" model predicted the temperature profile within concrete using data already established from conventional fire curves. However, this approach can only be used on buildings that have been subjected to temperatures within the normal time-temperature curve. The " Residual Area Method " employed a further method. This approach yields a set of formulae for calculating the critical temperature in the steel profile. **(Kodur and Agrawal, 2016)** give a technique for determining the residual capacity of RC beams exposed to fire was presented. The suggested method is achieved with the help of a comprehensive numerical model created in the finite element application ABAQUS. The numerical analysis predictions have a high agreement with the response parameters observed in experiments for assessing the residual capacity of RC beams subjected to fire. **(Mansur, et al., 1992)** proposed a rigorous method to calculate the deflection of beams with openings. In this methodology, the rafter is considered as a structural member with multiple segments that make up the solid parts and the sections crossed by the opening. Crack width is one of the major serviceability requirements of concrete structures, concrete's low tensile strength leads to crack occurrence in reinforced concrete under service loads. Cracking control is essential for the acceptable appearance and durability of concrete structures, particularly those subjected to an aggressive environment **(Carino, N. J., and Clifton, J. R., 1995)**. The ACI 318M-1995 code **(ACI 318R-95)** considered that the permissible maximum crack widths at service stages for exterior and interior exposure conditions are 0.3mm and 0.4mm, respectively. **(Mohammed, S. D., and Fawzi, N. M., 2016)** studied the influence of fire flame on the behavior of reinforced concrete beams affected by repeated load. Nine self-compacted reinforced concrete beams were castellated; all have the same geometric layout (0.15x0.15x1.00)

m, reinforcement details, and compressive strength (50 Mpa). To estimate the effect of fire flame disaster, four temperatures were adopted (200, 300, 400, and 500) ^{o}C, and two methods of cooling were used (graduated and sudden). As a comparison with the non-burned beam, the results indicated that the ultimate load capacity of the tested beams was reduced by (16, 23, 54, and 71) % after being burned to (200, 300, 400, and 500) ^{o}C, respectively, for a case of sudden cooling and by (8, 14, 36 and 64)%, respectively, for a case of graduated cooling. It was also found that the effect of sudden cooling was greater than that in the case of graduated cooling. **(Izzat, A. F., 2015)** investigated the performance of CFRP wrapping jackets used for retrofitting twelve square reinforced concrete (CR) column specimens damaged by exposure to fire flame, at different temperatures of 300, 500, and 700ºC, except for two specimens that were not burned. The ultimate load capacity of each retrofitted specimen was increased compared to that before retrofitting by about 16, 34, and 44% for the specimens burned at 300, 500, and 700ºC respectively, and cooled gradually. In contrast, this increase was 44% and 111% for the specimens subjected to burning temperatures of 500 and 700ºC, respectively, but cooled suddenly.

2. Beams set up

The variables which had been chosen in this work included the number and configuration of the openings, in addition to the burning temperature. All rafters had the same length, width, heights, reinforcement, and the load was centered at the midpoint after burning. **Fig. 1** shows the details of the rafters. All beams were identically reinforced, as shown in **Figs. 2** and **3**. The beam was examined in a simple scheme with an effective span of 2.8 m. The examined rafters are divided into three groups that were formed based on heating temperature (room temperature, 400 °C, and 700 °C), with each group consisting of four rafters (solid, rafters with 6 and 8 trapezoidal openings, and rafters with eight circular openings). **Table 1** and **Fig. 1** show the details of the tested rafters. **Fig. 2** and **3** show the configuration of the test specimens and the schematic diagrams of the reinforcement arrangement of the reference and other reinforced concrete NPRC beams.
Normal concrete has been used for pouring beams. The properties of normal concrete and steel reinforcements (at elevated temperature) used in this work are shown in **Table 2**.

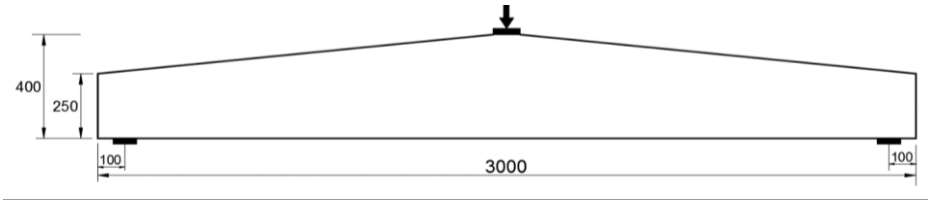

Solid non-prismatic beams GB, GB-400, and GB-700

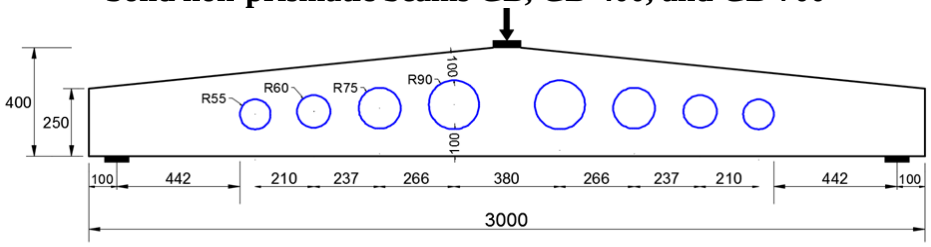

Non-prismatic beams with circular openings shape GC8, GC8-400, and GC8-700

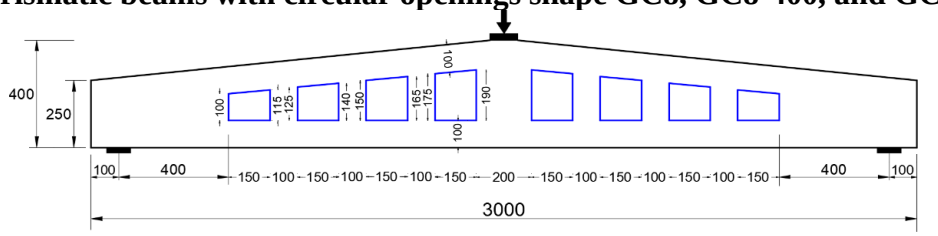

Non-prismatic beams with eight trapezoid openings GT8, GT8-400, and GT8-700

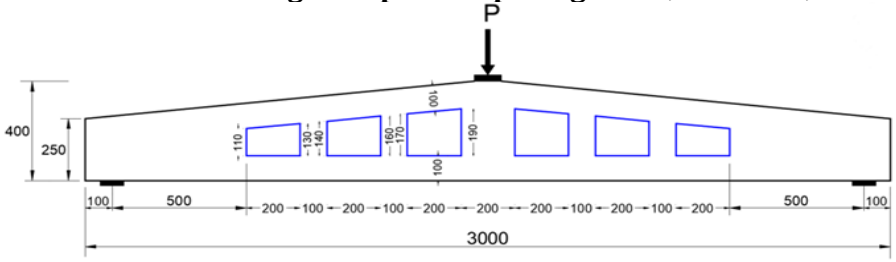

Non-prismatic beams with six trapezoid openings GT6, GT6-400, and GT6-700

Figure 1. Schematic layout of non-prismatic beams (every measure is in millimeters).

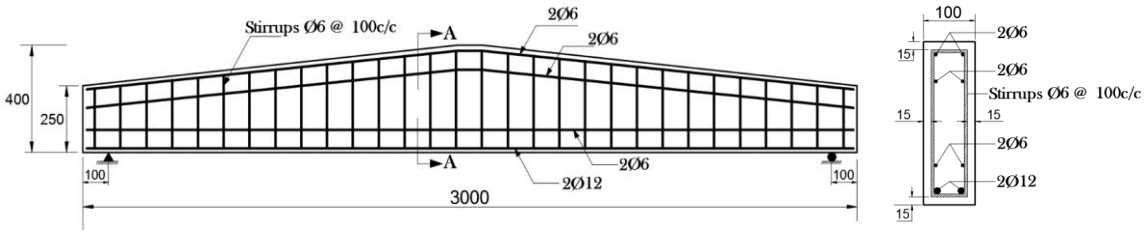

Details of steel reinforcement **Section A-A**

Figure 2. Details of steel reinforcement of GB, GB-400, and GB-700 (every measure is in millimeters).

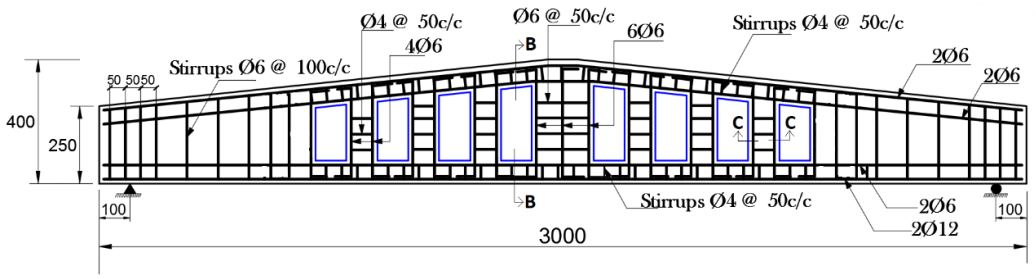

Figure 3. Details of steel reinforcement of perforated rafter (all dimensions are in mm)

Table 1. Details of tested rafters.

Group ID	Beams ID	Configuration of openings	No. of openings	The total area of opening (mm^2)	Width of openings (mm)	$\frac{weight_{rafter}}{weight_{GB}}$	Fire Temp. C°
Group I	GB	-	-	0	-	1.0	Ambient
	GC8	Circle-shaped	8	128000	0.83D	0.86	Ambient
	GT8	Trapezoid-shaped	8	174000	150	0.81	Ambient
	GT6	Trapezoid-shaped	6	180000	200	0.81	Ambient
Group II	GB-400	-	-	0	-	1.00	400
	GC8-400	Circle-shaped	8	128000	0.83D	0.86	400
	GT8-400	Trapezoid-shaped	8	174000	150	0.81	400
	GT6	Trapezoid-shaped	6	180000	200	0.81	400
Group III	GB-700	-	-	0	-	1.00	700
	GC8-400	Circle-shaped	8	128000	0.83D	0.86	700
	GT8-700	Trapezoid-shaped	8	174000	150	0.81	700
	GT6	Trapezoid-shaped	6	180000	200	0.81	700

Table 2. Materials properties.

Material	Ø (mm)	Yield stress (MPa)			Compressive strength (MPa)			Ultimate tensile strength (MPa)			Modulus of elasticity (GPa)		
		Amb.	400	700	Amb.	400	700	Amb.	400	700	Amb.	400	700
Concrete	--	--	--	--	32.6	25	12.6	--	--	--	26.86	20.1	13.1
Steel	4	390	352	262	--	--	--	590	547	456	200	200	194
	6	580	524	390	--	--	--	650	602	503	200	200	194
	12	610	570	496	--	--	--	722	657	549	200	200	194

3. Burning stage:

The burning process was conducted in a furnace (0.8x2x3.5m) manufactured specially for this test. The rate of the period of transition to achieve the target temperature 400 and 700°C was 7 and 10 minutes, respectively approximately similar to the rate of **ASTM E-119, 2016**, the exposure period of 1.0 hr after achieving the target temperature as shown in **Fig. 4.**

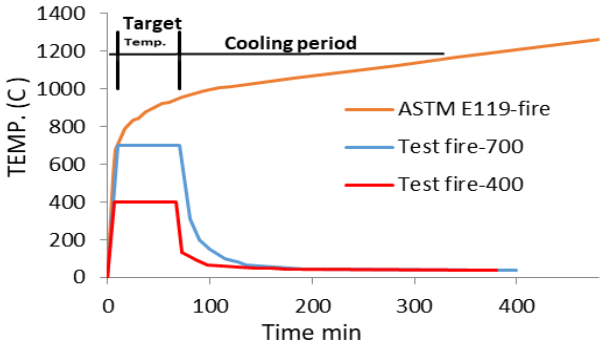

Figure 4. Fire scenarios used in the burning test

4. Deflection

Table 3 represents two attempts to calculate mid-span deflections depending on the experimental data regarding the following equation

$$\delta = \frac{P.L^3}{48 \times E\ I} \quad (1)$$

Where

P = 40kN (closer to the average of serviceability load) applied at mid-span of 2800mm,

E = concrete modulus of elasticity at each exposure temperature of 400 and 700°C (**Table 2**), and **I** is the moment of inertia of transformed cracked section calculated using two proposed methods. It was proposed that the cross-section dimensions at the quarter length of the gable (non-prismatic) beam can be used to calculate the average moment of inertia whereas, the other method depends on dividing the perforated gable into segments depending on the existing openings. Moment of inertia is calculated as demonstrated below:

The cross-section dimensions at the quarter length of the gable (non-prismatic) beam can be used to calculate the average moment of inertia whereas, and the other method depends on dividing the perforated gable into segments depending on the existing openings, as shown in **Fig. 5** as follows:

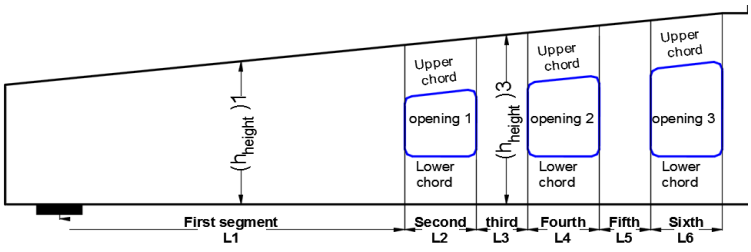

Figure 5. Segmental rafter method.

The height at any distance (h_x) can be calculated from the following equation (**Fig. 6**):

$$h_x = h_o\left(1 - \frac{x}{L_1}\right) + \frac{x}{L_1} h_1 \quad (2)$$

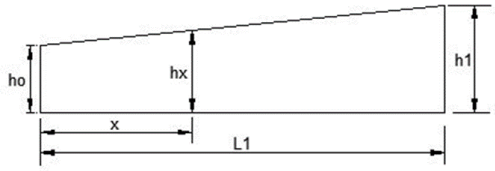

Figure 6. Schematic layout of a gable beam.

1-I at quarter of span of solid rafter (GB)

Quarter of span length = 750 mm

$h_x = 326 \rightarrow d = h_x - 37 = 289$ mm

$\rho = As/bd = 0.009809$, $n = 7.44 \rightarrow \rho n = 0.07298$

$$k = \sqrt{2\rho n + (\rho n)^2} - \rho n \quad (3)$$

k= 0.31597

kd =91 mm

$I_{cr} = 100*(91)^3/3 + 7.44*226(298-91)^2 + 7.44*56.5(247-91)^2 = 107394425$ mm^4

2-I of perforated rafter GT6, for example

Figure 7 shows the method of calculation of moment of inertia of transformed cracked sections depending on the segmental rafter method

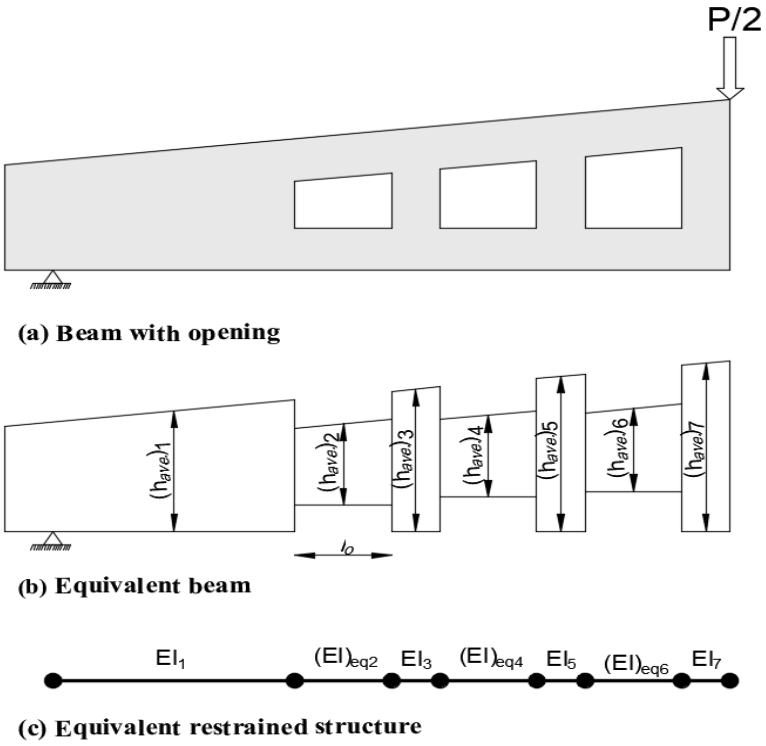

Figure 7. Equivalent segmented beam.

The First attempt was conducted by using the moment of inertia recommended by some references for solid gable rafters and reduced for those with openings by the ratio of residual rafter self-weight. Then, using **Eq. 1, the** deflection was calculated.

Second, it was performed by using the moment of inertia of transformed cracked sections depending on the segmental rafter method as follows:

$$I = [\, I_{first\ segment} \times \frac{L1}{L} + I_{2(opening1)} \frac{L2}{L} + I_{3(post)} \frac{L3}{L} + \cdots]. \quad (4)$$

Table 3. Experimental and calculated mid-span deflection of rafters at 40 kN.

Beam ID	*Ec*	*Experimental Deflection*	**The residual self-weight**					***The proposed segmental method***		
			Self-weight reduction	*Residual Self-weight(1)*	*I at quarter of span (2)*	*Calculated Deflection*	*Def exp. / def. calculated (%)*	*Moment of inertia (I) (3)*	*Calculated Deflection(4)*	*Def exp. / def. calculated (%)*
GB	26860	6.4	0	1	107394425	6.34	100.9	107394425	6.34	100.9
GT6	26860	9.96	19.5	0.805	86452512	7.87	126.4	62322000	10.92	91.14
GT8	26860	8.36	18.8	0.812	87204273	7.80	107	63471000	10.73	78
GC8	26860	6.51	13.9	0.861	92466600	7.36	88.3	82920331	8.21	79.2
GB-400	20153	8.32	0	1	107394425	8.45	98.4	107394425	8.45	98.4
GT6-400	20153	13.76	19.5	0.805	86452512	10.50	131.0	62322000	14.56	94.4
GT8-400	20153	11.61	18.8	0.812	87204273	10.41	111.5	63471000	14.30	81.1
GC8-400	20153	11.06	13.9	0.861	92466600	9.81	112.6	82920331	10.94	101
GB-700	13100	10.4	0	1	107394425	13	80	107394425	13	80
GT6-700	13100	19.78	19.5	0.805	86452512	16.2	122	62322000	22.4	88.3
GT8-700	13100	18.12	18.8	0.812	87204273	16	113	63471000	22	82.4
GC8-700	13100	13.12	13.9	0.861	92466600	15.1	87	82920331	16.84	78
			Average				106	Average		87.74
			S.D.				16.1	S.D.		9.1
			COV				15.1	COV		10

(1) Residual Self-weight = (100- Self-weight reduction)/100
*(2) Moment of inertia at quarter span * Residual Self-weight (1)*
(3) Moment of inertia calculation appendix A by using the proposed segmental method.

Table 3. reveals deflection calculated using the first attempt (self-weight reduction) converging to the experimental data. In contrast, the second attempt (segmental rafter method) converged to the experimental mid-span deflection for post-fire rafters exposed to 400 and 700ºC, and it was acceptable for those unexposed.

5. Maximum crack width

The flexural crack width at the service stage can be calculated according to control requirements in ACI 318M-1995 code, using the following form:

$$w = 0.011\beta\, f_s \sqrt[3]{d_c\, A_O} * 10^{-3}\ mm \qquad (5)$$

And $w = 2\frac{fs}{Es}\beta\sqrt{d_c^2 + (\frac{s}{2})^2}$ (6)

where:

$\beta = \frac{h-x}{d-x}$ = the ratio of distances between extreme tension face and neutral axis to distance between the neutral axis and centroid of reinforcing steel; β = 1.20 in rafters may be used to compare the crack widths gained in flexure and axial tension.

$f_s = n \times \frac{M\,c}{I}$ = stress in the tension reinforcement calculated on the basis of a cracked section (N/mm^2),

n = modular ratio = E_s / E_c , c=d-x.
d_c = the distance measured from the centroid of tensile steel to the extreme tensioned fiber
$A_o = \frac{2\,d_c\,b}{n_b}$ = the area of concrete surrounding each reinforcing bar,
n_b =the number of tensions reinforcing bars**,**
b = width of the section**, s**= maximum bar spacing.

Using **eq. 6** from **(Nilson, et al., 2016)** for calculation, the crack width of rafter exposure to fire is better than **eq. 5** because of existing the modulus of elasticity of steel in the denominator of this equation

Table 4 shows the comparison between the experimental crack width and the calculated one (according to **eq. 6**) under the load =30 kN.

Load versus maximum crack width curves for rafters are presented in **Figures. 8, 9** and **10**. From **Fig. 10** it's obvious that flexural crack width increased with increasing the burning temperature.

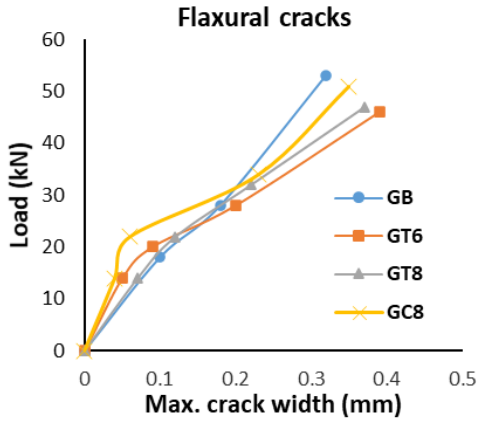

a- **Flexural crack width for group ambient**

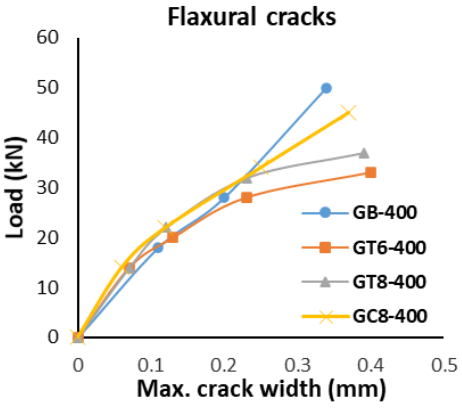

b- **Flexural crack width for Group 400**

Figure 8. Load versus maximum crack width (flexural cracks) till service stage for Groups ambient and 400.

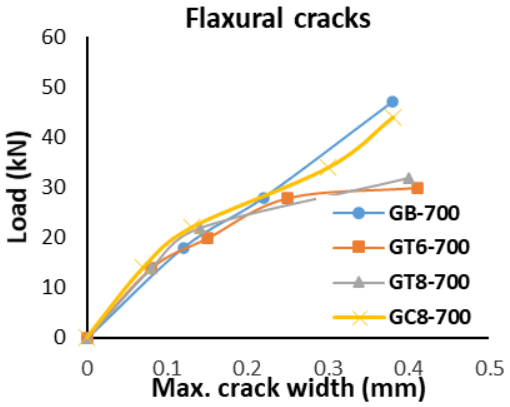

c- Flexural crack width for Group 700

Figure 9. Load versus maximum crack width (flexural cracks) till service stage for Groups ambient 700.

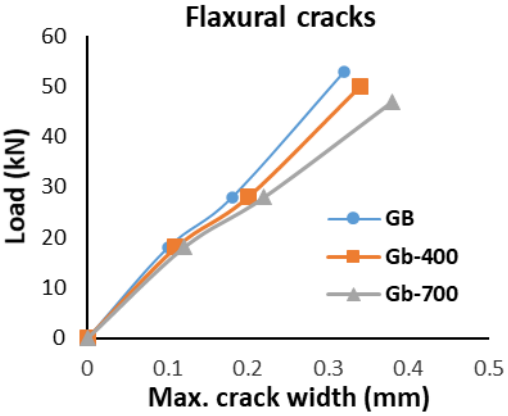

a-Flexural crack width for a solid group

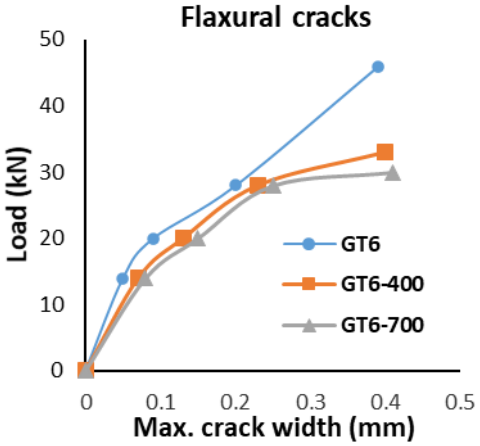

b-Flexural crack width for GT6 Group

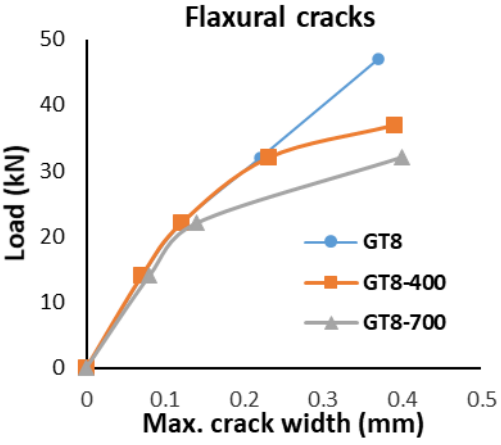

c-Flexural crack width for GT8 Group

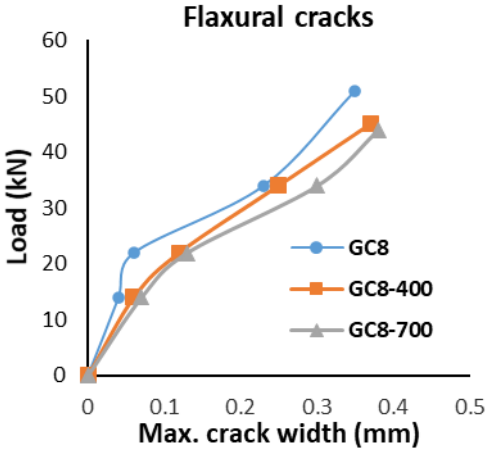

d-Flexural crack width for GC8 Group

Figure 10. Load versus maximum crack width curves (flexural cracks) till service stage for GB, GT6, GT8, and GC8 groups.

Table 4. A comparison between the experimental crack width and the calculated one.

Beam - ID	Moment (N.mm)	Moment of inertia (mm^4)	n=Es/Ec	fs (MPa)	Fs=<fy(610)	Es (MPa)	w_p=calculated crack width (mm)	W_e = experimental crack width (mm)	We/Wp (%)
GB	21000000	107394425	7.44	386.9	386.9	200000	0.175	0.191	109
GT6	21000000	62322000	7.44	666.8	610	200000	0.276	0.221	80
GT8	21000000	63471000	7.44	654.7	610	200000	0.276	0.212	76.8
GC8	21000000	82920331	7.44	501.2	501.2	200000	0.2268	0.21	92.6
GB-400	21000000	107394425	9.92	515.9	515.9	200000	0.2335	0.212	90.8
GT6-400	21000000	62322000	9.92	889.1	610	200000	0.276	0.232	84
GT8-400	21000000	63471000	9.92	873	610	200000	0.276	0.228	82.6
GC8-400	21000000	82920331	9.92	668	610	200000	0.276	0.226	81.9
GB-700	21000000	107394425	14.87	773.4	610	194800	0.283	0.236	83.3
GT6-700	21000000	62322000	14.87	1332.8	610	194800	0.283	0.47	165.8
GT8-700	21000000	63471000	14.87	1308	610	194800	0.283	0.395	139.4
GC8-700	21000000	82920331	14.87	1001	610	194800	0.283	0.25	88.2
							Mean = 98		
							SD = 27.4		
							COV = 28		

6. CONCLUSIONS

1- Deflection calculated using the first attempt (self-weight reduction) converges to the experimental data, in contrast to the second attempt (segmental rafter method). The average experimental to calculated deflection percentage was 1.06 for the first method and 0.877 for the second method.

2- Deterioration and cracks were observed on the rafter's concrete surfaces after exposure to high temperatures. These cracks expanded and increased in width with increasing the burning temperature.
3- The maximum crack width calculated using eq. 6 converges to the experimental data where the average percentage of experimental to calculated maximum crack width was 0.98.
4- The flexural crack width increased with increasing the burning temperature.

REFERENCES

- ACI Standard: Commentary on Building Code Requirements for Structural Concrete (ACI 318R-95), 1995.
- ASTM, E., 2016. ASTM E119-16a. Standard Test Methods for Fire Tests of Building Construction and Materials," ASTM International, West Conshohocken, PA: 21.
- Chang, Yun-Fei, Yih-Houng Chen, Maw-Shyong Sheu, and George C Yao. 2006. Residual stress-strain relationship for concrete after exposure to high temperatures, *Cement and Concrete Research*, 36: 1999-2005.
- Darwin, D., Dolan, C. W., and Nilson, A. H., 2016. *Design of concrete structures*, (Vol. 2). New York, NY, USA: McGraw-Hill Education.
- GEORGALI, B., and TSAKIRIDIS, P. 2005. Microstructure of fire-damaged concrete. A case study, *Cement and Concrete composites*, 27, 255-259.
- Handoo, SK, S Agarwal, and SK Agarwal. 2002. Physicochemical, mineralogical, and morphological characteristics of concrete exposed to elevated temperatures, *Cement and Concrete Research*, 32: 1009-18.
- Hassan, Maryam Abdul Jabbar, Amer Farouk Izzet, and Nazar K Oukaili. 2020. Structural Performance Under Monotonic Static Loading of Reinforced Concrete Gable Roof Beams with Multiple Web Openings, *International Journal of Civil Engineering*: 1-20.
- Izzat, A. F., 2015. Retrofitting of Reinforced Concrete Damaged Short Column Exposed to High Temperature, *Journal of Engineering*, 21(3), 34-53.
- Kodur, VKR, and Ankit Agrawal, 2016. An approach for evaluating residual capacity of reinforced concrete beams exposed to fire, *Engineering Structures*, 110: 293-306.
- Lee, Jaesung, Yunping Xi, and Kaspar Willam. 2008. Properties of concrete after high-temperature heating and cooling, *ACI Materials Journal*, 105: 334.
- Mansur, M. A., Huang, L. M., Tan, K. H., and Lee, S. L., 1992. Deflections of Reinforced Concrete Beams with Web Openings, *ACI Structural Journal*, V. 89, No. 4, 1992.
- Mohammed, S. D., and Fawzi, N. M., 2016. Fire Flame Influence on the Behavior of reinforced Concrete Beams Affected by Repeated Load. *Journal of Engineering*, 22(9), 206-223.
- Carino, N. J., and Clifton, J. R., 1995. Prediction of Cracking in Reinforced Concrete Structures, Building and Fire Research Laboratory, *National Institute of Standards and Technology*, 1995.

- Tufail, Muhammad, Khan Shahzada, Bora Gencturk, and Jianqiang Wei, 2017. Effect of elevated temperature on mechanical properties of limestone, quartzite and granite concrete, *International Journal of Concrete Structures and Materials*, 11: 17.
- WANG, Z.-H., and TAN, K. H., 2006. Residual area method for heat transfer analysis of concrete-encased I-sections in fire. *Engineering Structures*, 28, 411-422.

- WICKSTROM, U., 1986. A very simple method for estimating temperature in fire exposed concrete structures. *Technical Report SP-RAPP* ,45, Swedish National Testing Institute.